Observations of Saharan dust layer electrification

2011 Environ. Res. Lett. 6 014001

(http://iopscience.iop.org/1748-9326/6/1/014001)

Environ. Res. Lett. **6** (2011) 014001 (7pp) doi:10.1088/1748-9326/6/1/014001

Observations of Saharan dust layer electrification

K A Nicoll[1], R G Harrison[1] and Z Ulanowski[2]

[1] Department of Meteorology, University of Reading, PO Box 243, Earley Gate, Reading, Berkshire RG6 6BB, UK
[2] Science and Technology Research Institute, University of Hertfordshire, Hatfield AL10 9AB, UK

Received 16 September 2010
Accepted for publication 2 December 2010
Published 23 December 2010
Online at stacks.iop.org/ERL/6/014001

Abstract
Electrification of atmospheric dust influences the coagulation, wet removal and fall speeds of dust particles. Alignment of dust particles can also occur in fair weather atmospheric electrical conditions if the particles are charged. However, very few electrical measurements made in elevated dust layers exist. Balloon-borne charge and particle instrumentation have been used to investigate the electrical properties of elevated Saharan dust layers. Soundings from the Cape Verde Islands, which experience frequent Saharan dust outbreaks, intercepted several dust layers. Two balloon soundings during summer 2009 detected dust particles in layers up to 4 km altitude. Simultaneous electrical measurements showed charge inside the dust layers, with a maximum measured charge density of 25 pC m^{-3}, sufficient to influence wet removal processes.

Keywords: aerosol electrification, Cape Verde, Martian dust, atmospheric aerosol

1. Introduction

Dust is known to be an important constituent of planetary atmospheres which influences the transfer of radiation to and from the planet [1]. On Earth, the Sahara desert is the most important source of atmospheric mineral dust, with annual emissions estimated to be several hundred megatons per year [2]. The dust is carried in the local atmospheric circulation, mostly arising from lofting in desert regions through erosion and meteorological processes. Mineral dust particles can be transported over long distances from their source region, modifying the radiative balance of the undisturbed atmosphere by scattering and absorbing both long and shortwave radiation [3].

Charge presents a potential complicating factor in the radiative impact of mineral dust. This occurs in several ways. Firstly, charging of dust particles affects the dynamics of particles, particularly small particles. Secondly, charging also affects droplet–particle scavenging processes [4], and therefore the removal of dust by cloud droplets. Recently, electrical alignment of dust particles above the surface has also been suggested [5]. Astronomical polarimeter measurements by Ulanowski *et al* [5] found that dust particles were vertically aligned, which decreases the optical thickness of the dust layer, as the reduced cross section of the aligned particles allows more solar radiation to pass through the layer, similar to Venetian blinds. Particle alignment is neglected in conventional models of the atmospheric radiative effects of dust clouds, hence if it is abundant, atmospheric radiative calculations may need to be modified from the existing random orientation assumption. Likewise, alignment can alter the angular scattering properties of dust layers, including both unpolarized and polarized radiances, which influences remote sensing retrievals of dust properties, particularly from satellite platforms [6]. Dust particle alignment is thought to be caused by electrical effects [5], similar to vertical alignment of ice crystals observed by radar near the tops of thunderstorms [7] where large electric fields of ∼10–100 kV m^{-1} are present.

Previous surface atmospheric electric field measurements during violent dust storms were ∼3 kV m^{-1} [8, 9], and up to 100 kV m^{-1} within dust devils [10, 11], but there are very few measurements of charge in more passive dust layers, particularly aloft. For a layer of uncharged dust particles, an increase in the atmospheric electric field within an elevated dust layer occurs from ion–aerosol attachment, whereby small ions are lost to the larger aerosol particles [12, 13] decreasing the air conductivity. In one of the few previous dust electricity measurements, Gringel and Mülheisen [14] measured the

electrical conductivity with a balloon-borne Gerdien condenser through an elevated layer of Saharan dust at 3 km altitude. The dust layer conductivity was a factor of four smaller than its clear air value at the same height.

To investigate particle charging in dust layers aloft, simultaneous detection of dust particles and charge in a suitable dust layer is required. This paper describes co-located measurements of dust and charge inside elevated dust layers using a specially developed meteorological balloon sounding system, obtained during a field campaign in the Cape Verde Islands.

2. Methodology

In situ measurements of dust size, abundance and electrification were made using an adapted meteorological radiosonde, which carried additional science sensors to measure dust size and concentration (an aerosol particle counter) and charge (a dust charge sensor), as explained below, followed by data analysis in section 3.

2.1. Instrumentation

The dust charge sensor (DCS) consists of a 12 mm diameter spherical metal electrode, connected to an electrometer voltmeter [15]. Charge is induced in the DCS electrode and transferred to it directly by impacts from electrified particles, changing the electrode voltage. The electrode voltage is reset every 60 s, and the rate of change of electrode voltage, along with the ascent rate of the sonde, used to determine the local charge density during each measurement cycle. A drift correction was also applied. Determination of polarity from the DCS is ambiguous where particles are present, due to a combination of impaction and induction, therefore only the charge density magnitude is reported. The sensor was calibrated in the lab by the induction effect, generating a range of changing electric fields in the absence of impaction effects; these are expected to be small as substantial particle charges are required to produce detectable voltage changes. Uncertainties in the derived charge density result from a geometrical (capacitance) factor determined by lab calibration, the ascent rate, and deriving the rate of change of electrode voltage [16].

The aerosol particle counter (APC) measures particle size and number concentration using light scattered from particles drawn into a sampling chamber by an air pump. The APC detects particles in five different size bins, with minimum particle diameters of 0.6, 1.4, 2.6, 5.4, 10.6 μm, and measures a maximum particle concentration of a few 10^6 particles per litre [17]. The APC was calibrated in the laboratory using standard aerosol particles. Uncertainties in the APC measurements arise from difficulties in characterizing the sampling efficiency of the counter during flight. In a previous comparison of the APC measurements with sun photometer data from an AERONET site during a campaign, the integrated size distribution derived from the APC data agreed to within a factor of two of that from AERONET.

The DCS and APC were flown alongside a Vaisala RS92 standard digital meteorological radiosonde which measures pressure, temperature, relative humidity and GPS position information. The extra instrumentation was interfaced to the RS92 using a programmable data acquisition system (DAS) originally developed for the RS80 analogue radiosonde [18], which enabled the DCS and APC data to be sent synchronously with the meteorological data. Measurements were made at 1 Hz, which, for a typical mean balloon ascent rate of 4 m s^{-1}, gave nominally 4 m vertical resolution.

2.2. Location and chronology

The DCS and APC sensors were flown during a two week field campaign in the Cape Verde Islands. The Cape Verde Islands, off the west coast of Africa, experience frequent dust events originating from the Sahara desert. Seasonal variation in the vertical distribution of dust over the islands leads to substantial dust concentration near the surface in winter, but several kilometres above the surface in summer [19]. This is due to the seasonal shift of the inter-tropical convergence zone; during summer, dust is transported above the trade winds in the so-called Saharan air layer, up to 5–7 km altitude [19]. Our field campaign in late August 2009 was when most dust events occurred above the boundary layer. Figure 1 shows the aerosol optical depth (AOD) at 550 nm derived from the MODIS instrument on the Terra satellite during the week of the field campaign from 23rd to 30th August. Over the Cape Verde Islands, the AOD was high ~0.6, demonstrating the presence of sustained dust outbreaks from the north-west coast of Africa during this period.

3. Charged dust measurements

Balloon launches were from Sal (22°57 W, 16°45 N—location with respect to the west coast of Africa is shown in figure 2) one of the easterly islands, where standard meteorological radiosondes are launched at 1200 GMT. Four instrumented balloon launches were made from Sal, and two are described here. All balloons carried an APC, DCS, and the RS92 radiosonde: the instruments were not recovered after each flight.

The soundings of interest—in terms of intercepted dust—took place on 26/08/09 and 29/08/09, and their trajectories are plotted in figure 2. Both sondes travelled west from Sal, over the ocean. During the 26/08/09 sounding, the sonde reached 21 km, with descent data to within 2.5 km of the surface (including GPS data), after travelling 67 km horizontally. The 29/08/09 sounding reached 24 km, with descent data to within 1 km. However, only science data was obtained during the descent, as the GPS signal was lost at 11 km on the ascent.

3.1. Sounding A—29th August

Figure 3 shows vertical profiles of (a) meteorological parameters—temperature and relative humidity (RH), and (b) total aerosol particle concentration and charge density from the descent stage of the flight. Using the descent, after the balloon bursts, ensures no possibility of contamination of the APC sampling from balloon wake effects. Figure 3(b) shows two distinct layers of aerosol at 4 and 2 km, with maximum

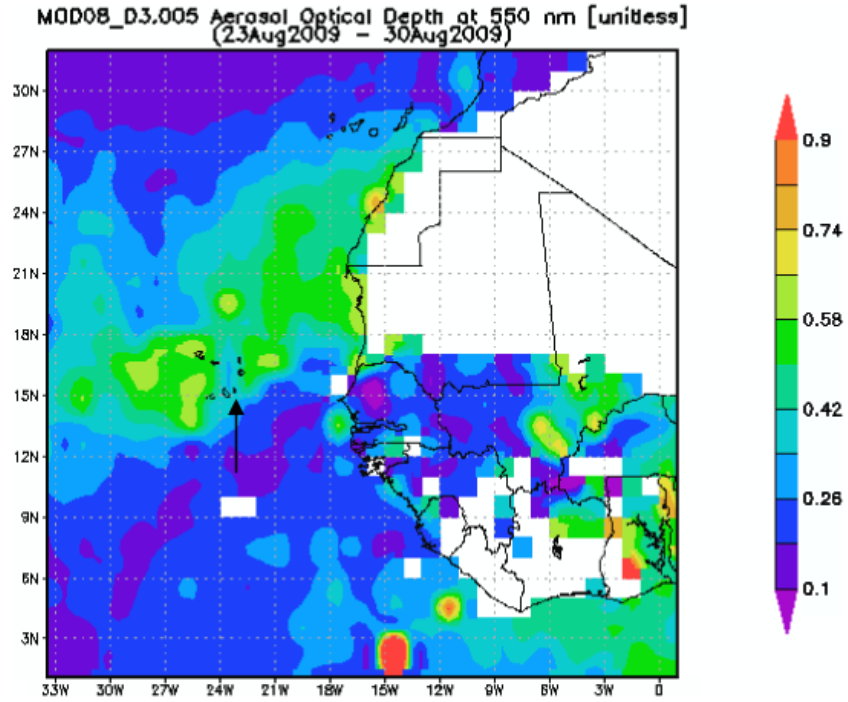

Figure 1. Aerosol optical depth at 550 nm from 23rd to 30th August 2009 near the west coast of Africa, as measured by the MODIS instrument on the Terra satellite. The location of the Cape Verde Islands is given by the black arrow. Image generated by the Giovanni data viewer at http://gdata2.sci.gsfc.nasa.gov/daac-bin/G3/gui.cgi?instance_id=aerosol_daily.

particle concentrations of ∼12 particles cm^{-3}. The black lines represent the total particle concentration, which is the sum of the aerosol particle concentration in all five of the size bins. 95% of the particles detected were in the smallest size bin (diameters between 0.6 and 1.4 μm); the remaining 5% were in the range 1.4–2.6 μm. During the initial lofting stage, the dust layer would probably have contained larger particles, with diameters of tens of micrometres [8], however due to the layer age, larger particles would have settled out before reaching Cape Verde. (A 25 μm diameter particle initially at 4 km reaches the ground by gravitational settling within one day.) Dust over the Cape Verde Isles is also evident on the 1442 UTC lidar image from the CALIPSO satellite on 29/08/09, which shows dust from the surface up to an altitude of ∼5 km [20].

Also evident in figure 3(b) are two layers of charge, coincident with the aerosol layers. Maximum charge densities of ∼5 pC m^{-3} are present in each layer. The upper layer occurs at a similar height to the temperature inversion at 3.8 km in figure 3(a), not inconsistent with charged dust being trapped beneath the inversion.

3.2. Sounding B—26th August

Charged dust was also detected on the 26/08/09 sounding. Measurements made by a sun photometer on Sal (part of the AERONET network) confirm the presence of dust in the atmosphere, as the median AOD from 1100 to 1600 GMT was 0.6 (at 675 nm) on 26/08/09. By comparison, the AOD was only 0.21 during the same time period on 24/08/09.

Figure 4 shows vertical profiles of (a) temperature and RH and (b) total aerosol particle concentration and charge density for sounding B. As for figure 3, the data is from the descent, thus the vertical profile does not include the surface as the radiosonde signal was lost at 2.5 km. Figure 4(b) shows a distinct layer of aerosol with its upper edge at ∼3.8 km, and maximum particle concentration of 60 particles cm^{-3}, much denser than the aerosol layer measured in sounding A. All of the detected particles were contained within the two smallest size bins, with 88% of the measured particle diameters between 0.6 and 1.4 μm and 12% of the particle diameters between 1.4 and 2.6 μm. The red circles in figure 4(b) show a charge layer at approximately the same height as the aerosol layer, with a maximum charge density of 25 pC m^{-3}. The maximum in charge density is near the upper edge of the aerosol layer at 3.8 km. Within the aerosol layer itself the variability in the charge density is much larger than that in the clear air above, demonstrating the presence of charged aerosol particles within the layer. Also seen in figure 4(b) is a secondary aerosol layer at 4.2 km, which too is coincident with a region of charge. The RH profile in figure 4(a) demonstrates that, although the RH throughout the dust layers was fairly high (∼70%), the air was unsaturated, hence the layer observed was not cloud.

4. Discussion

The measurements described in figures 3 and 4 show that charge is present where particles are observed, for two soundings through layers of Saharan dust. These results support qualitatively the hypothesis of charging in elevated dust layers, which is now examined quantitatively.

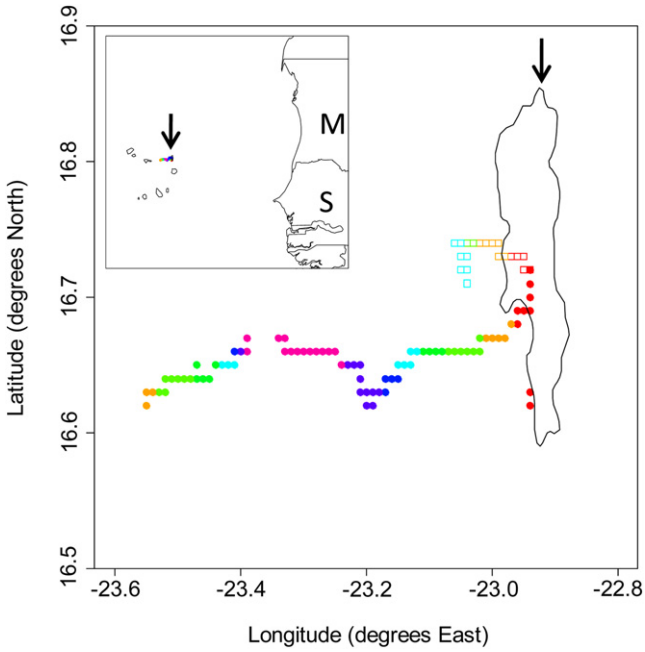

Figure 2. Inset—location of the Cape Verde Islands in relation to the west coast of Africa. The arrow denotes the position of the island of Sal, and M represents Mauritania, and S, Senegal. Main plot—trajectory of two of the instrumented sonde soundings, launched from Sal. Solid circles denote the trajectory of the sonde flight on 26/08/09 (sounding B), and hollow squares, the trajectory on 29/08/09 (sounding A), where position data was lost due to a poor GPS signal. Points are coloured according to height, where red denotes 0–3 km, yellow 3–4.5 km, green 4.5–8 km, blue 8–13 km, purple 13–16.5 km, and pink 16.5–20 km.

4.1. Quantitative considerations

A quantitative comparison can be made by examining the distribution of charge density in the 'clear air' and 'dust laden air' from each of the two soundings. Figure 5 presents histograms, by sounding, of particle concentration and charging. 'Clear air' charge density was selected on the basis of particle concentration being zero, and 'dust laden air' was denoted by particle concentration >1 cm^{-3}. In both soundings, the median charge density in dust laden air was larger than in clear air, demonstrating that the dust layers were electrically charged with respect to the surrounding air. For sounding A, the median 'clear air' charge density was 0.7 pC m^{-3}, and the 'dust laden air' 1.0 pC m^{-3}; whilst for sounding B, the median 'clear air' charge density was 0.2 pC m^{-3} and the 'dust laden air' 0.7 pC m^{-3}. The Mann–Whitney test [21] was used to test for differences in the distributions of charge data between clear and dust laden air from the two soundings. Using the test, for sounding A, the two distributions were marginally statistically different ($p = 0.05$), and for sounding B, the two distributions were significantly different ($p \ll 0.05$).

Both results support the existence of charge in the dust layers, as for the 'dust laden air' distributions, the criterion used to select charge measurements was very strict. This is because the DCS will respond to distant charged particles through induction, as well as by direct impact. In contrast, particles must physically enter the APC inlet before they are detected, thus some of the larger charge density values may have occurred before dust particles had been sampled.

4.2. Dust charging mechanisms

The DCS responds to the total charge density, which is carried on particles and small ions. In a dust layer it is likely that the ion concentration is low, due to ion–particle attachment, therefore charge will principally be carried on the dust particles.

Individual particle charging can occur during the lofting stage due to particle–particle collisions, and collisions with the surface. Granular charging in the atmosphere can occur by several mechanisms. One theory argues that neutral particles become charged by initial polarization from a strong external electric field, and transfer their charge through subsequent collisions [22]. This theory requires large electric fields for particle charging, but an atmospheric electric field is

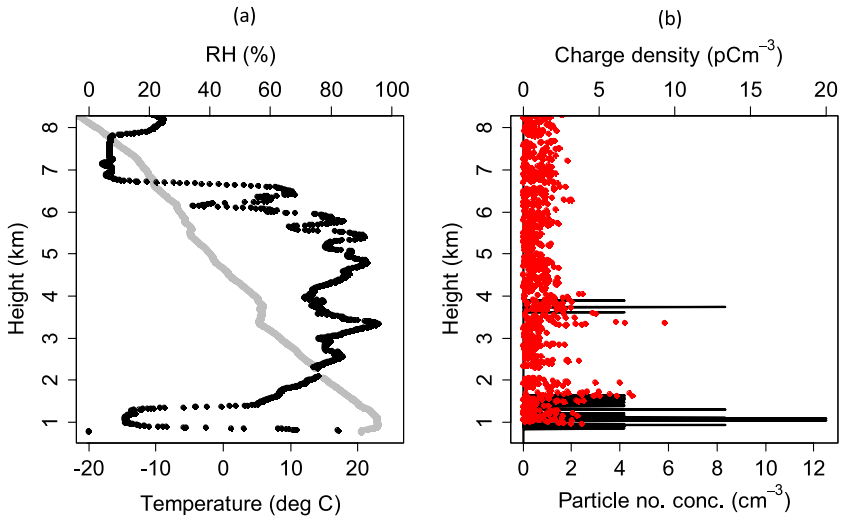

Figure 3. Vertical profile of (a) temperature (grey) and relative humidity, RH (black), (b) total aerosol particle number concentration (black lines) and magnitude of charge density (red points) measured on sounding A (29/08/09), west of Sal, Cape Verde. Launch time—1130 GMT.

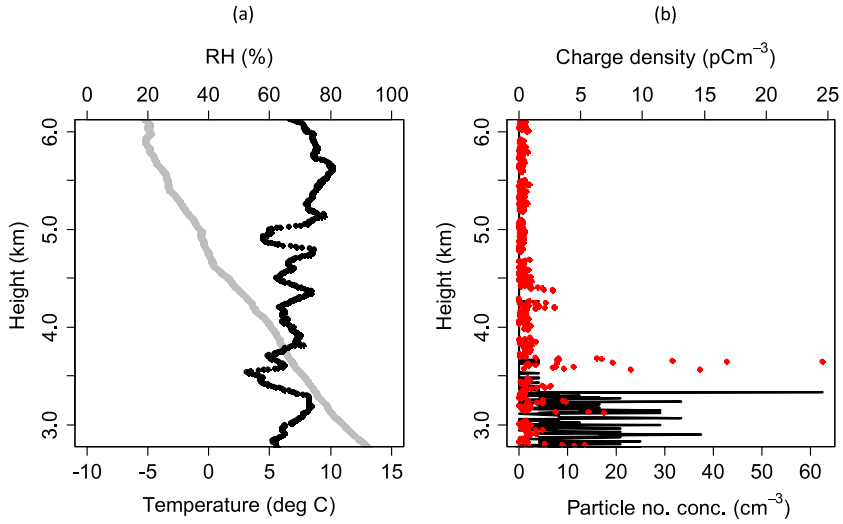

Figure 4. Vertical profile of (a) temperature (grey) and relative humidity, RH (black), (b) total aerosol particle number concentration (black lines) and magnitude of charge density (red points) measured on sounding B (26/08/09), west of Sal, Cape Verde. Launch time—1130 GMT.

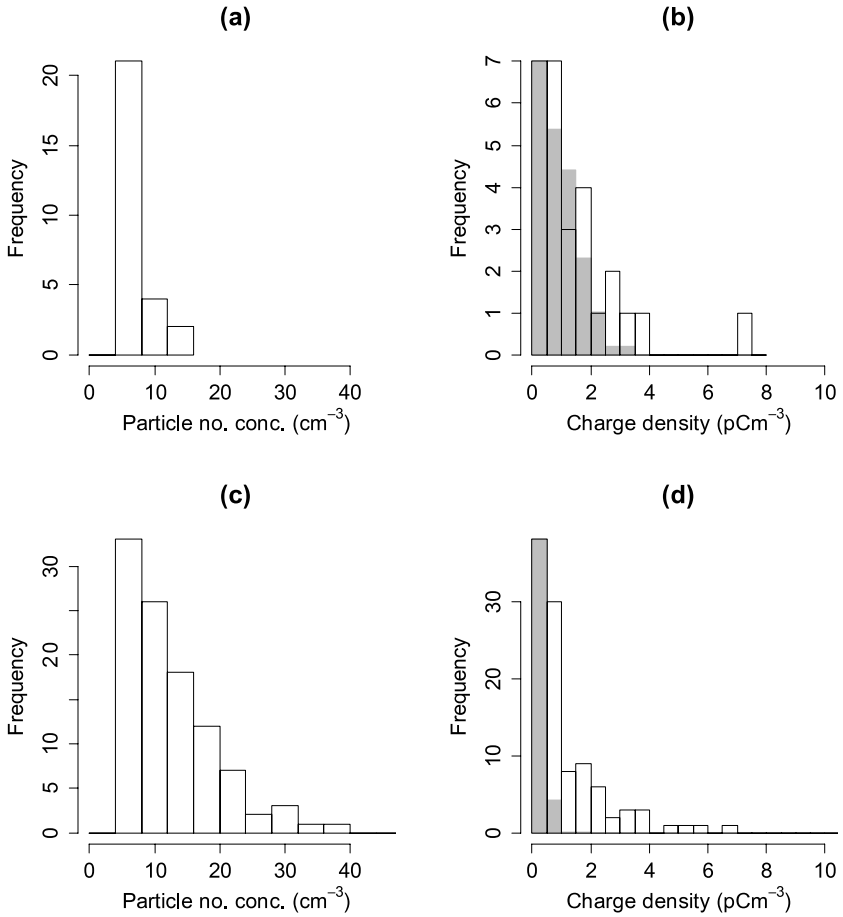

Figure 5. Histograms of particle number concentration for all dust layers per sounding, ((a) and (c)), and histograms of the magnitude of 'clear air' and 'dust laden air' charge densities for each sounding ((b) and (d)). (a) and (b) represent sounding A, and (c) and (d) sounding B. The grey bars in (b) and (d) represent the 'clear air' charge density and hollow bars the charge density measured in 'dust laden air'.

always present in fair weather [23], which would be enhanced locally by the reduced air conductivity in a dust cloud [24]. Further charging mechanisms which explain the triboelectric charging of chemically identical particles have been identified theoretically [25, 26], and also experimentally [27], which may also play a role in the electrification of atmospheric dust.

A known mechanism by which individual dust particles charge occurs at the dust layer edge, from vertical electric

current flow in the global electric circuit as it passes through particle layers [28]. Flow of the 'conduction current' through a conductivity gradient, such as near dust layer edges generates layers of charge density [29]. Such charge layers have been found near stratified liquid water cloud edges [28], and a stratified aerosol layer will produce a similar conductivity transition to that of cloud. Figure 4(b) shows a large increase in the charge density at the upper dust layer edge at 3.6 km. The charge density in this region is much larger than for the bulk of the layer, which indicates layer edge (global electric circuit) charging. Charge generated on the edges of aerosol layers can be mixed turbulently into the bulk of the layers, however mixing efficiency considerations suggest that charge in the middle of the layer will be much smaller than that near the edges. To estimate the dust layer edge charge, the particle number concentration can be used to derive the vertical gradient in conductivity, using the steady-state ion balance equation [28, 30]. Using this method, the charge density calculated for the dust layer upper edge at 3.6 km on 26/08/09 is 0.1 pC m^{-3}, much smaller than the 25 pC m^{-3} measured by the DCS. This suggests that fair weather edge charging alone is insufficient to account for the charge observed, as for the volcanic plume from the Eyjafjallajökull eruption [30].

With no charging mechanisms, the initial particle charge decays by ion–particle collisions. The charge relaxation timescale can be calculated using the ion balance equation in the ion–particle attachment limit [31]. Using the maximum measured particle number concentration from the sounding on 26/08/09 (62 cm^{-3}), and the median measured particle diameter of 1.1 μm, the relaxation time is 70 s, i.e. much shorter than the transit time from any local continental source. Seven day back-trajectories calculated by NASA [32], using AERONET data from Sal, show the sampled layer to have originated from north-west Africa at least two days previously; any initial charging at lofting would therefore have decayed through ion–particle interactions. The presence of non-zero charge density inside the dust layer therefore suggests a continuous particle charging mechanism.

4.3. Charge effects on dust particles

Charge affects particle motion and particle collection by droplets, as well as potentially particle alignment. A particle's weight can be compensated by a vertical electric force. For a vertical electric field of 500 V m^{-1} and spherical dust particles of density 2.65 g cm^{-3} and diameter 1.1 μm, 170e (elementary charges) are required. In terms of dust particle charge estimated from the DCS and APC during the Cape Verde field campaign, assuming that the measured charge density was solely from dust charge equally distributed, for Flight B, with the larger charges observed, the derived mean particle charge was 2e, and the maximum charge 37e. For the mean measured particle size, charges of magnitude 2e increase the collection efficiency by a factor of two, and 37e increases it by a factor of six [33]. Hence, the motion of particles is less likely to be affected than their ultimate collection by water droplets. In terms of electro-alignment, the charging observed is a pre-requisite for alignment, but the particles observed were smaller than those for which the previous alignment calculations were made [5]. Combined *in situ* electric field and polarization measurements remain necessary for confirmation.

5. Conclusions

These balloon-borne observations of charge and particles made in elevated dust layers near Cape Verde establish that the individual dust particles aloft are charged despite the slow charge relaxation expected in the conductivity of atmospheric air. Previous electrical measurements made near the surface in Saharan dust storms found charge densities of 0.3–30 nC m^{-3} [34, 9] however, we find that in Saharan dust layers well above the surface, charge is still present but the charge density is much less, with the maximum measured space charge 25 pC m^{-3}. Differences in the particle size distributions, number concentration and charging mechanisms between surface dust storms and elevated passive layers are expected, leading to differences in the measured charge densities. The surface and elevated circumstances therefore appear unlikely to be comparable quantitatively.

Acknowledgments

NERC supported the field campaign (DREAME project NE/G007268/1) and KAN through a studentship. Ester Brito and Jose Carlos from the Instituto National De Meteorologia the Instituto Nacional De Meteorologia E Geofisica, Sal, Cabo Verde assisted with balloon launches, and Reading and Hertfordshire technical staff helped with equipment logistics. The Terra MODIS image in figure 1 was acquired by NASA and generated by the Giovanni data viewer at http://gdata2.sci.gsfc.nasa.gov/daac-bin/G3/gui.cgi?instance_id=aerosol_daily. Tom L Kucsera (GEST) at NASA/Goddard generated the back-trajectories, available at http://aeronet.gsfc.nasa.gov, and Didier Tanri provided data from the Cape Verde AERONET site.

References

[1] Davies D W 1979 Effects of dust on the heating of Mars' surface and atmosphere *J. Geophys. Res.* **84** 8289–93
[2] Schütz L 1980 Long range transport of desert dust with special emphasis on the Sahara *Ann. New York Acad. Sci.* **338** 515–32
[3] Engelstaedter S, Tegen I and Washington R 2006 North African dust emissions and transport *Earth-Sci. Rev.* **79** 73–100
[4] Tinsley B A, Rohrbaugh R P, Hei M and Beard K V 2000 Effects of image charges on the scavenging of aerosol particles by cloud droplets and on droplet charging and possible ice nucleation processes *J. Atmos. Sci.* **57** 2118–34
[5] Ulanowski Z, Bailey J, Lucas P W, Hough J H and Hirst E 2007 Alignment of atmospheric mineral dust due to electric field *Atmos. Chem. Phys.* **7** 6161–73
[6] Ulanowski Z, Kalashnikova O V, Lucas P W and Bercot B 2008 Effect of charging on radiative and transport properties of atmospheric mineral dust *3rd Dust Workshop (Leipzig, 15–17 September 2008)*
[7] Saunders C P R and Rimmer J S 1999 The electric field alignment of ice crystals in thunderstorms *Atmos. Res.* **51** 337–43

[8] Williams E, Nathou N, Hicks E, Pontikis C, Russel I B, Miller M and Bartholomew M J 2008 The electrification of dust-lofting gust fronts ('haboobs') in the Sahel *Atmos. Res.* **91** 292–8
[9] Kamra A 1972 Measurements of the electrical properties of dust storms *J. Geophys. Res.* **77** 5856–69
[10] Jackson T L and Farrell W M 2006 Electrostatic fields in dust devils: an analog to Mars *IEEE Trans. Geosci. Remote Sens.* **44** 2942–9
[11] Renno N O *et al* 2004 MATADOR 2002: a pilot field experiment on convective plumes and dust devils *J. Geophys. Res.* **109** E07001
[12] Rycroft M J, Israelsson S and Price C 2000 The global atmospheric electric circuit, solar activity and climate change *J. Atmos. Sol.-Terr. Phys.* **62** 1563–76
[13] Rycroft M J, Harrison R G, Nicoll K A and Mareev E 2008 An overview of earth's global electric circuit and atmospheric conductivity *Space Sci. Rev.* **137** 83–105
[14] Gringel W and Mülheisen R 1978 Sahara dust concentration in the troposphere over the north Atlantic derived from measurements of air conductivity *Beitr. Phys. Atmos.* **51** 121–8
[15] Nicoll K A and Harrison R G 2009 A lightweight balloon-carried cloud charge sensor *Rev. Sci. Instrum.* **80** 014501
[16] Nicoll K A 2010 Coupling between the global electric circuit and clouds *PhD Thesis* University of Reading
[17] Ulanowski Z, Hirst E, Kaye P H, Harrison R G, Nicoll K A and Rogers G 2010 Radiosonde aerosol counter for vertical profiling of atmospheric dust layers *EGU General Assembly (Vienna, Austria)* p 13512
[18] Harrison R G 2005 Inexpensive multichannel digital data acquisition system for a meteorological radiosonde *Rev. Sci. Instrum.* **76** 026103
[19] Chiapello I, Bergametti G, Gomes L, Chatenet B, Dulac F, Pimenta J and Santos Suares E 1995 An additional low layer transport of Sahelian and Saharan dust over the north & eastern Tropical Atlantic *Geophys. Res. Lett.* **22** 3191–4
[20] http://www-calipso.larc.nasa.gov/products/lidar/browse_images/show_calendar.php
[21] Mann H B and Whitney D R 1947 On a test of whether one of two random variables is stochastically larger than the other *Ann. Math. Stat.* **18** 50–60
[22] Pahtz T, Herrmann H J and Shinbrot T 2010 Why do particle clouds generate electric charges? *Nat. Phys.* **6** 364–8
[23] Israel H 1971 Atmospheric Electricity (Jerusalem: Israel Program for Scientific Translations)
[24] Ette A I I 1970 The effect of the Harmattan dust on atmospheric electric parameters *J. Atmos. Terr. Phys.* **33** 295–300
[25] Lacks D J, Duff N and Kumar S K 2008 Nonequilibrium accumulation of surface species and triboelectric charging in single component particulate systems *Phys. Rev. Lett.* **100** 188305
[26] Kok J F and Lacks D J 2009 Electrification of granular systems of identical insulators *Phys. Rev.* E **79** 051304
[27] Forward K M, Lacks D J and Sankaran R M 2009 Charge segregation depends on particle size in triboelectrically charged granular materials *Phys. Rev. Lett.* **102** 028001
[28] Nicoll K A and Harrison R G 2010 Experimental determination of layer cloud edge charging from cosmic ray ionisation *Geophys. Res. Lett.* **37** L13802
[29] Tinsley B A 2000 Influence of solar wind on the global electric circuit, and inferred effects on cloud microphysics, temperature and dynamics in the troposphere *Space Sci. Rev.* **94** 231–58
[30] Harrison R G, Nicoll K A, Ulanowski Z and Mather T A 2010 Self-charging of the Eyjafjallajokull volcanic ash plume *Environ. Res. Lett.* **5** 024004
[31] Harrison R G and Carslaw K S 2003 Ion–aerosol–cloud processes in the lower atmosphere *Rev. Geophys.* **41** 1012
[32] Kucsera T L 2010 NASA/Goddard http://aeronet.gsfc.nasa.gov
[33] Tripathi S N, Vishnoi S, Kumar S and Harrison R G 2006 Computationally efficient expressions for the collision efficiency between electrically charged aerosol particles and cloud droplets *Q. J. R. Meteorol. Soc.* **132** 1717–31
[34] Oluwafemi C O and Ette A I I 1974 On the vertical distribution of space charge during the Harmattan *J. Geophys. Res.* **79** 871–2